

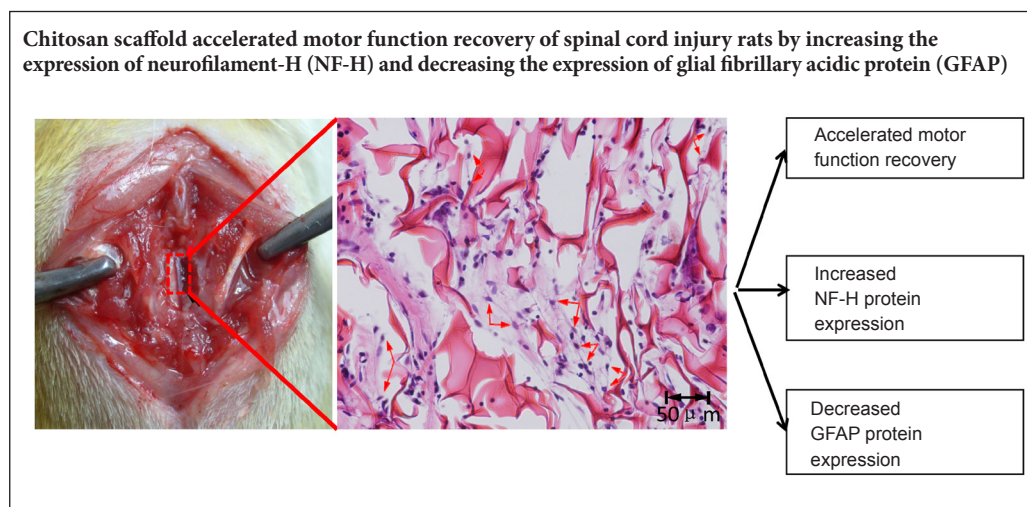
Efficacy of chitosan and sodium alginate scaffolds for repair of spinal cord injury in rats

Zi-ang Yao, Feng-jia Chen, Hong-li Cui, Tong Lin, Na Guo, Hai-ge Wu*

School of Life Science and Technology, Dalian University, Dalian, Liaoning Province, China

Funding: This work was supported by the National Natural Science Foundation of China, No. 81671243 and 81373429.

Graphical Abstract



*Correspondence to:

Hai-ge Wu, Ph.D.,

haige-hu@163.com.

orcid:

0000-0003-0412-0192

(Hai-ge Wu)

doi: 10.4103/1673-5374.228756

Accepted: 2017-12-25

Abstract

Spinal cord injury results in the loss of motor and sensory pathways and spontaneous regeneration of adult mammalian spinal cord neurons is limited. Chitosan and sodium alginate have good biocompatibility, biodegradability, and are suitable to assist the recovery of damaged tissues, such as skin, bone and nerve. Chitosan scaffolds, sodium alginate scaffolds and chitosan-sodium alginate scaffolds were separately transplanted into rats with spinal cord hemisection. Basso-Beattie-Bresnahan locomotor rating scale scores and electrophysiological results showed that chitosan scaffolds promoted recovery of locomotor capacity and nerve transduction of the experimental rats. Sixty days after surgery, chitosan scaffolds retained the original shape of the spinal cord. Compared with sodium alginate scaffolds- and chitosan-sodium alginate scaffolds-transplanted rats, more neurofilament-H-immunoreactive cells (regenerating nerve fibers) and less glial fibrillary acidic protein-immunoreactive cells (astrocytic scar tissue) were observed at the injury site of experimental rats in chitosan scaffold-transplanted rats. Due to the fast degradation rate of sodium alginate, sodium alginate scaffolds and composite material scaffolds did not have a supporting and bridging effect on the damaged tissue. Above all, compared with sodium alginate and composite material scaffolds, chitosan had better biocompatibility, could promote the regeneration of nerve fibers and prevent the formation of scar tissue, and as such, is more suitable to help the repair of spinal cord injury.

Key Words: nerve regeneration; spinal cord injury; chitosan; sodium alginate; functional recovery; scaffold; neurofilament-H; glial fibrillary acidic protein; scar tissue; locomotor capacity; neural regeneration

Introduction

Spinal cord injury (SCI), as a major issue threatening human health, can cause patients to suffer from serious sensory and movement dysfunction (Sun et al., 2016). Every year, many patients suffer from SCI due to traffic accidents or other external trauma, and often leads to systemic or partial paralysis, and even death (Figueiredo et al., 2017). In spite of the growing knowledge of SCI processes, the treatments available for these patients are still unsatisfactory (Austin et al., 2017). Traumatic injury to the adult mammalian spinal cord causes irrevocable damage, producing an environment that inhibits regrowth of damaged axons (Bolsover et al., 2008). Studies have shown that damaged axons can regenerate and allow partial origi-

nal nerve conduction function with appropriate therapeutic interventions and a suitable microenvironment (Subramanian et al., 2009; Kim et al., 2014; Rabchevsky et al., 2017). Appropriate tissue engineering scaffolds implanted in the damaged spinal cord can improve the microenvironment, promote the repair of SCI, and provide a possible solution to overcome SCI problems (Li et al., 2016; Wen et al., 2016; Ding et al., 2017). Chitosan and sodium alginate are both marine polysaccharides, and many studies have shown that they have good biocompatibility and biodegradability (Austin et al., 2012; Liu and Zhao, 2013; Cheung et al., 2015), and are suitable to be used as biomaterials to aid the recovery of damaged tissue (Nunamaker et al., 2007; Saravanan et al.,

2016).

To study the nerve repair functions of chitosan and sodium alginate, chitosan scaffolds, sodium alginate scaffolds and composite scaffolds (chitosan-sodium alginate scaffolds) were prepared and implanted into rats with SCI. The nerve repair functions of the three kinds of scaffolds were then evaluated by the recovery of locomotor capacity and nerve conduction, scar tissue formation and nerve fiber regeneration at the SCI sites.

Materials and Methods

Animals

Forty-eight female Wistar rats (250–280 g) were purchased from the Experimental Animal Center of Dalian Medical University of China (certification No. SCXK (Liao) 2008-0002) and maintained in a standard animal room for 1 week before experiments. The study protocol was approved by the Animal Ethics Committee of Dalian University of China (approval No. dlu2016022).

Preparation of chitosan scaffolds

Chitosan was purchased from Fuli Biotechnology Co., Ltd., Hangzhou, China. The deacetylation degree of chitosan used was 95%, and its average molecular weight was 1,000 kDa. The chitosan scaffolds were prepared as follows: 0.15 g chitosan was dissolved in 10 mL 1% acetic acid solution and left to stand until air bubbles disappeared. The chitosan solution was then injected into a 24-well plate using a syringe and maintained in place without stirring to remove bubbles. After air bubbles were completely gone, the 24-well plate with chitosan solution was frozen at -20°C , then dried by freeze drying. The obtained chitosan sponge was cut into $2 \times 2 \times 4 \text{ mm}^3$ blocks, immersed in 5% NaOH solution for 10 minutes and then washed with distilled water until they were at neutral pH. The chitosan scaffolds were sterilized with ultraviolet light for 1 hour.

Preparation of sodium alginate scaffolds

Sodium alginate was obtained from Sinopharm Chemical Reagent Shanghai Co., Ltd., Shanghai, China. Its average molecular weight was approximately 74 kDa, and the mannuronic (M)/guluronic acid (M/G) ratio was approximately 1.7. The preparation method for sodium alginate scaffolds was similar to that of chitosan scaffolds. The obtained $2 \times 2 \times 4 \text{ mm}^3$ sodium alginate sponges were separately put into 50 mM CaCl_2 and 200 mM NaCl solution for 30 minutes, then washed three times with distilled water. After freeze drying, the sodium alginate scaffolds were sterilized with ultraviolet light for 1 hour.

Preparation of composite material (chitosan-sodium alginate) scaffolds

The $2 \times 2 \times 4 \text{ mm}^3$ sodium alginate sponges were prepared as above and separately put into 50 mM CaCl_2 and 200 mM NaCl solution for 30 minutes. After the sponges were washed three times with 0.2 M sodium acetate/acetic acid buffer (pH 4.2), they were put into 1% chitosan (dissolved in 0.2 M sodium acetate/acetic acid buffer (pH 4.2)) for 24 hours,

to allow adequate reaction time to form chitosan-sodium alginate scaffolds. Afterwards, the chitosan-sodium alginate scaffolds were separately washed three times with 0.2 M sodium acetate/acetic acid buffer (pH 4.2) and distilled water. After freeze drying, the composite material scaffolds were sterilized with ultraviolet light for 1 hour.

Observation of the surface structure of scaffolds with a scanning electron microscope (SEM)

The scaffolds were glued to the conductive tape of the sample holder, and exposed to evaporated gold. The scaffolds were observed with an SEM (S-4800; Hitachi, Tokyo, Japan) and photographed.

Establishment of SCI models

All 48 female Wistar rats were anesthetized by intraperitoneally injecting 6% chloral hydrate (0.5 mL/100 g body weight). Laminectomy was performed at the level of T_{9-10} . A quantitative SCI mold (length 4 mm, width 1.5 mm) was inserted into the incision of the dura mater. The spinal cord within the mold was extracted. As the spinal cord at this level is 3 mm in diameter (Waibl, 1973), the dissected spinal cord segment represented approximately half of the spinal cord across its width from the right side, and the remaining half of the spinal cord on the left side was left intact. Thus, the hemisection spinal cord model was set up. The 48 female Wistar rats were randomly divided into control, chitosan scaffold, sodium alginate scaffold and composite material scaffold groups, with 12 rats per group. The mold was taken out and the different scaffolds were implanted into the lesion site. For the control group, the same operation was performed without implantation. The muscles and skin were sutured with degradable sutures. Immediately after the operation, the rats were administered 4 mL warm saline intraperitoneally to supplement the loss of blood and body fluids during surgery. After the surgery, 200,000 U penicillin was injected subcutaneously into the rats once daily for 3 days. The bladder was massaged twice daily after surgery until normal bladder function was restored.

Behavioral assessment

To evaluate the degree of recovery of locomotor capacity after SCI, the Basso-Beattie-Bresnahan (BBB) locomotor rating scale (Basso et al., 1995) was used, which ranges from complete paralysis (score 0) to normal locomotion (score 21). This was carried out by two observers blinded to the design of the experiment and surgery groups. The test was carried out every three days until 60 days after surgery using an open field. Each rat was observed three times by two observers separately, and the mean of six observation scores was calculated.

Electrophysiological testing

Sixty days after surgery, the somatosensory evoked potentials (SEP) of experimental rats were detected with an electromyography-evoked potentiometer (Medcom Technology, Zhuhai, China). SEP testing conditions: the recording electrode was inserted into the T_{8-9} interspinous ligament. The refer-

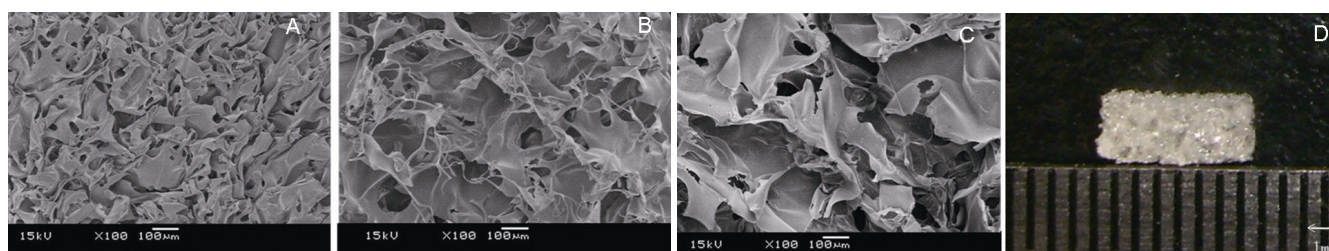


Figure 1 Surface structure of the three kinds of scaffolds as shown by scanning electron microscopy (original magnification, 100×). (A–C) Surface structure of (A) chitosan scaffolds, (B) sodium alginate scaffolds, (C) chitosan-sodium alginate scaffolds, scale bars in A–C: 100 μm. (D) The size of the scaffolds is shown. Scale bar: 1 mm. The size of all scaffolds was 2 × 2 × 4 mm³. The surface structure of the chitosan scaffold was compact and porous, that of the sodium alginate scaffold was looser, and that of composite material scaffold was loosest.

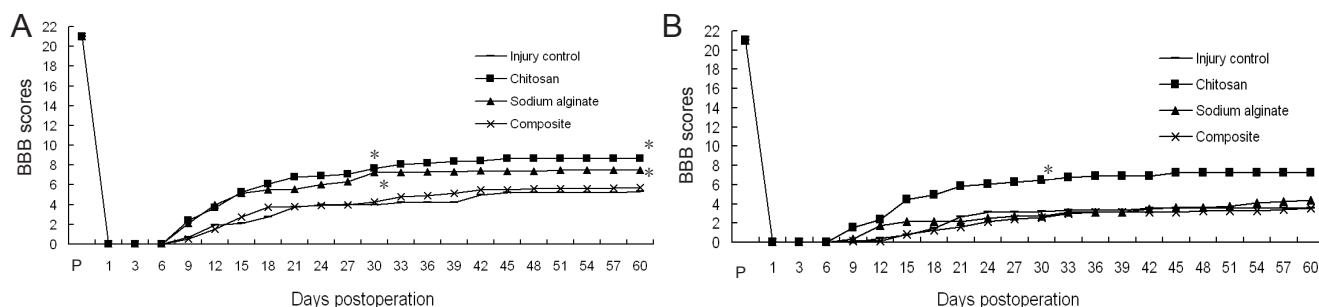


Figure 2 BBB locomotor rating scale scores of left and right hind limbs of rats from the four groups.

(A) Right hind limb (the injured side); (B) left hind limb (the un-operated side). Forty-eight female Wistar rats were used to establish the hemisection spinal cord injury model. No scaffold or chitosan, sodium alginate, or chitosan-sodium alginate composite scaffolds were implanted into the injury site of the rats. One day after surgery, two observers blinded to the design and surgery of the experiment carried out the BBB locomotor scoring of experimental rats until 60 days after surgery. Each rat was separately observed three times by two observers, and the mean of six observation scores was calculated (mean ± SD, $n = 12$, one-way analysis of variance followed by the Student-Newman-Keuls *post hoc* test; * $P < 0.05$, vs. injury control group). Chitosan: Chitosan scaffold group; sodium alginate: sodium alginate scaffold group; composite: composite material scaffold group; BBB: Basso-Beattie-Bresnahan scale.

ence electrode was 0.5 cm from the recording electrode. The stimulating electrode was inserted into the subcutaneous tibial nerve of the medial ankle of experimental rats. Quivering of the ankle and toes was observed at a stimulation intensity of 2.5 mA and stimulation frequency of 2 Hz.

Immunohistochemistry and hematoxylin-eosin staining

Sixty days after surgery, the rats were anesthetized by intraperitoneally injecting 6% chloral hydrate (0.5 mL/100 g body weight) and the spinal cord was excised after cardiac perfusion with 4% paraformaldehyde dissolved in 0.1 M phosphate buffered saline. The excised spinal cord was fixed in 4% paraformaldehyde for an additional 12 hours. The injury site was observed under a dissecting microscope (BX41; Olympus, Tokyo, Japan) and photographed. The fixed spinal cord including the injury site was embedded in paraffin after dehydration, and the paraffin was cut into 15 μm thick longitudinal sections. Sections of the same position were selected to stain with hematoxylin and eosin and photographed using a microscope imaging system. After dewaxing and antigen retrieval, sections at the same position were incubated with monoclonal mouse anti-neurofilament-H (NF-H) antibody (1:100; Santa Cruz Biotechnology, Santa Cruz, CA, USA) or monoclonal mouse anti-gial fibrillary acidic protein (GFAP) antibody (1:100; Santa Cruz Biotechnology) at 4°C overnight. The sections were incubated with biotinylated secondary antibody for 30 minutes and peroxidase-labeled streptavidin for 20 minutes. Antigen localization was visual-

ized by reaction with diaminobenzidine and examined using a microscope imaging system (BX41; Olympus). Three rats of each group were used for the quantitative analysis. Three longitudinal sections from each rat and three fields of each section were selected randomly to count and quantitate the level of positive staining (optical density) with Image-Pro Plus 6.0 software (Media Cybernetics, Rockville, MD, USA).

Statistical analysis

Data are expressed as the mean ± SD. All statistics were analyzed using SPSS 17.0 software (SPSS, Chicago, IL, USA). Differences between groups were compared by one-way analysis of variance followed by the Student-Newman-Keuls *post hoc* test. A value of $P < 0.05$ was considered statistically significant.

Results

Surface structures of various scaffolds after implantation

The photographs of the scaffold surface structures under SEM are shown in Figure 1. As shown in Figure 1D, the size of the scaffolds was 2 × 2 × 4 mm³. The scaffolds were porous sponges that had good stability in water. As shown in Figure 1A, the surface structure of chitosan scaffolds was compact and porous, and the diameter of each pore was approximately 15 μm. There were approximately 200 pores that could be observed in a 100× SEM photograph. The surface structure of sodium alginate scaffolds was also porous (Figure 1B), but the diameter of each pore was approximately 60 μm. Approximately 50 pores could be observed in a 100× SEM photograph. The

surface structure of composite material scaffolds (**Figure 1C**) was looser than that of sodium alginate scaffolds, and the diameter of each pore was approximately 100 μm . There were approximately 30 pores in a 100 \times SEM photograph.

Effects of different scaffolds on the recovery of locomotor capacity in SCI rats

Most rats experienced urinary incontinence and some rats had hematuria and urinary retention after the operation. Most of these rats recovered to normal urination within two weeks. Eight rats died after the operation. Among these, three rats were from the control group, one rat from the chitosan scaffold group and four rats from the composite material scaffold group.

Figure 2A shows the BBB score of the right hind limb (lesioned side) for the four groups. The locomotor capacity recovery of chitosan scaffold group rats began from day 6 after surgery and they recovered faster from day 6 to day 24. The other three groups of rats showed slow right hind limb locomotor recovery from day 9 after surgery. At 60 days after surgery, the average BBB score of the right hind limb in the chitosan scaffold group was approximately 7. This means that all three joints of the right hind limb could broadly function. However, the average BBB scale score of the right hind limb for the other three groups of rats was 3–4.5. Compared with the other three groups, the locomotor recovery in the chitosan scaffold group was improved significantly ($P < 0.05$). Compared with the control group, the BBB score of the right hind limb in the sodium alginate scaffold and composite material scaffold groups showed no significant differences ($P > 0.05$).

Figure 2B shows the BBB score of the left hind limb (unoperated side) in the four groups. The locomotor capacity recovery of all rats began from day 6 after surgery and recovered quickly from day 6 to day 24. At 60 days after surgery, the average BBB score of the left hind limb in the chitosan scaffold group was approximately 8, which means that under non load-bearing circumstances, the paw palmar surface of the left hind limb could touch the ground. The average BBB score of the left hind limb in the sodium alginate scaffold group was approximately 7, which means that all three joints of the left hind limb were broadly functional. The average BBB score of the left hind limb for the composite scaffold and control groups was approximately 5, which means that only one joint of the left hind limb was broadly functional. Compared with the control group, the locomotor capacity recovery in the chitosan scaffold and sodium alginate scaffold groups was more obvious ($P < 0.05$), but the difference between the chitosan scaffold and sodium alginate scaffold groups was not significant ($P > 0.05$).

Effects of different scaffolds on nerve conduction function in SCI rats

Figure 3 shows the SEP detection results. Compared with the control group, the SEP latency (including positive waves and negative waves) was shorter in the chitosan scaffold and sodium alginate scaffold groups but longer in the composite

material scaffold group. The SEP amplitude (including positive waves and negative waves) was enhanced in the chitosan scaffold and sodium alginate scaffold groups but reduced in the composite material scaffold group. The results showed that nerve conduction of the spinal cord was improved in the chitosan scaffold and sodium alginate scaffold groups. Moreover, the improvement in nerve conduction was more significant in the chitosan scaffold group than in the sodium alginate scaffold group.

Effects of different scaffolds on histological changes in SCI rats

At 60 days after surgery, the spinal cord was excised after cardiac perfusion. The injury site was observed under a dissecting microscope (**Figure 4**). There was apparent atrophy at the injury site of control rats (**Figure 4A**). In the chitosan scaffold group, spinal cord shape was well-maintained. The boundaries between spinal cord tissue and scaffold were blurred (**Figure 4B**). There was atrophy at the injury site and the boundary between spinal cord tissue and scaffold was clear in the sodium alginate scaffold group (**Figure 4C**). Swelling was seen at the injury site and the boundary between spinal cord tissue and scaffold was clear in the composite material scaffold group (**Figure 4D**).

Hematoxylin-eosin staining results are shown in **Figure 5**. The 40 \times microphotographs showed that the spinal cord of control rats was apparently atrophied (**Figure 5Aa**). At 200 \times magnification, many glial cells (round, small and light-colored) were obvious at the injury sites of control rats (black arrows), with extensive connective tissue and scarring (the tight tissue contained many glial cells), which seriously hampered axon extension at the injury site (**Figure 5Ba**). The chitosan scaffold was dyed pink by hematoxylin-eosin staining. The scaffold and spinal cord connected closely, and the spinal cord shape was well-maintained, with slight atrophy (**Figure 5Ab**). Compared with the control group, there were less glial cells and scarring around the chitosan scaffold and lesion (**Figure 5Bb**). **Figure 5Be** is an enlargement of part of **Figure 5Bb**. There were fibrous tissues or even neural networks within the chitosan scaffold (blue arrows), reflecting extension of nerve fibers into the scaffold. The sodium alginate scaffold degraded rapidly, and almost no scaffold was observed 60 days after surgery. Thus, the spinal cord was apparently atrophied and there were large holes (**Figure 5Ac**) and a great amount of scarring (**Figure 5Bc**, black arrows) at the injury site. The degradation rate of composite material scaffolds was slower than that of sodium alginate scaffolds due to the mixing of chitosan. There were large holes within the composite material scaffold and the connection of scaffold and spinal cord was loose (**Figure 5Ad**). Many cells were observed within the pores. Compared with the chitosan scaffold group, many more glial cells and fewer nerve fibers were observed (**Figure 5Bd**). Similar to the results from the dissecting microscope, the chitosan scaffold had better tissue compatibility and could maintain the spinal cord shape better, compared with the other two scaffolds.

Figure 6A shows the immunohistochemical results for

GFAP. In the control group, many GFAP-immunoreactive cells were observed at the injury site. A clear and coherent boundary was formed by GFAP-immunoreactive cells along the boundary of the lesioned area. Almost no GFAP-immunoreactive cells were observed at the injury site of rats from the chitosan scaffold group. The boundary formed by GFAP-immunoreactive cells along the boundary of the lesioned area was discontinuous compared with control rats. This means that chitosan scaffolds could prevent the scar from entering the damaged spinal cord. In the sodium alginate scaffold and

composite material scaffold groups, more GFAP-immunoreactive cells were observed at the injury site compared with the chitosan scaffold group. **Figure 6B** shows the quantitative results obtained by randomly selecting three fields of immunohistochemistry in microphotographs. GFAP expression at the injury site was obviously decreased in the chitosan scaffold group compared with the other three groups.

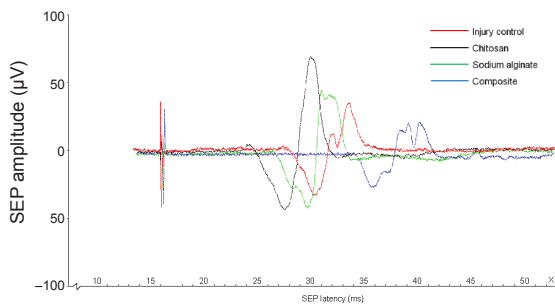


Figure 3 SEP waveforms in experimental rats from each group. Forty-eight female Wistar rats were used to establish the hemisection spinal cord injury model. Chitosan, sodium alginate, chitosan-sodium alginate composite or no scaffolds were implanted into the injury site of the rats. Sixty days after surgery, the SEP of experimental rats was detected with an electromyography-evoked potentiometer. Stimulation intensity is 2.5 mA and stimulation frequency is 2 Hz. The detection was stopped when the ankle joint and toes of the rats vibrated slightly. Control: Control group; chitosan: chitosan scaffold group; sodium alginate: sodium alginate scaffold group; composite: composite material scaffold group. SEP: Somatosensory evoked potential.

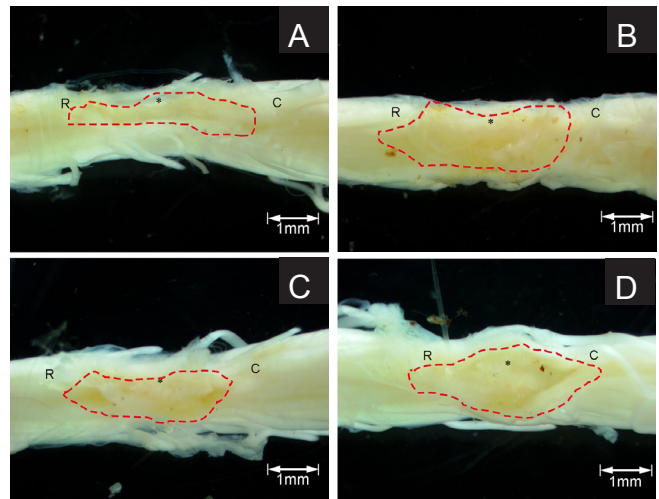


Figure 4 Spinal cord injury site of experimental rats 60 days after surgery. No scaffold (A), chitosan (B), sodium alginate (C) or chitosan-sodium alginate composite (D) scaffolds were implanted into the injury site of the rats. Sixty days after surgery, the spinal cords were excised and fixed in 4% paraformaldehyde. The injury site was observed under a dissecting microscope and photographed. Dotted lines indicate the boundary of the injury site. *: Injury center; R: rostral; C: caudal.

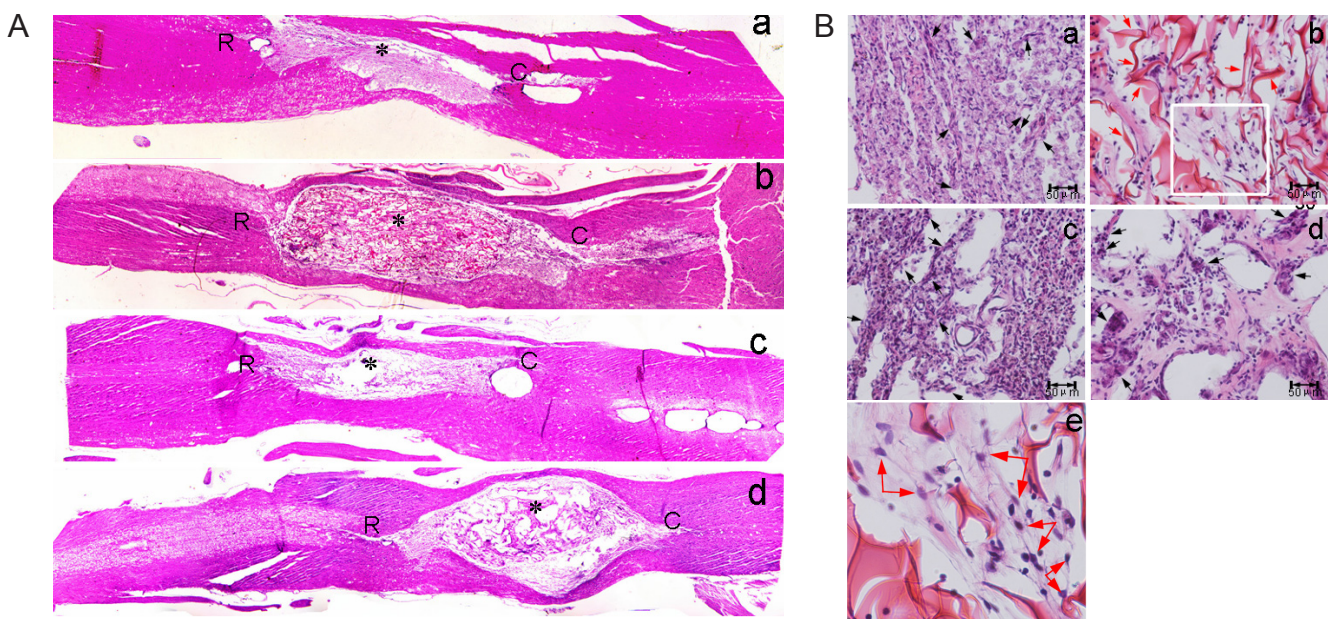


Figure 5 Hematoxylin-eosin staining of the spinal cord injury site of experimental rats 60 days after surgery. (A) Overall state of the injury site (original magnification, 40 \times); (B) sections at the injury site (original magnification, 100 \times (a–d), 200 \times (e)). Forty-eight female Wistar rats were used to establish the hemisection spinal cord injury model. No scaffold (a), chitosan scaffold (b), sodium alginate scaffold (c) or chitosan-sodium alginate composite scaffold (d) were implanted into the injury site of the rats. Sixty days after surgery, the spinal cords were excised, fixed, embedded in paraffin and stained with hematoxylin and eosin. The sections were photographed under a dissecting microscope. In A, * represents the injury center; R: rostral; C: caudal. In B, e is an enlargement of the box in b. The black arrows point to scar tissue and red arrows point to nerve fibers.

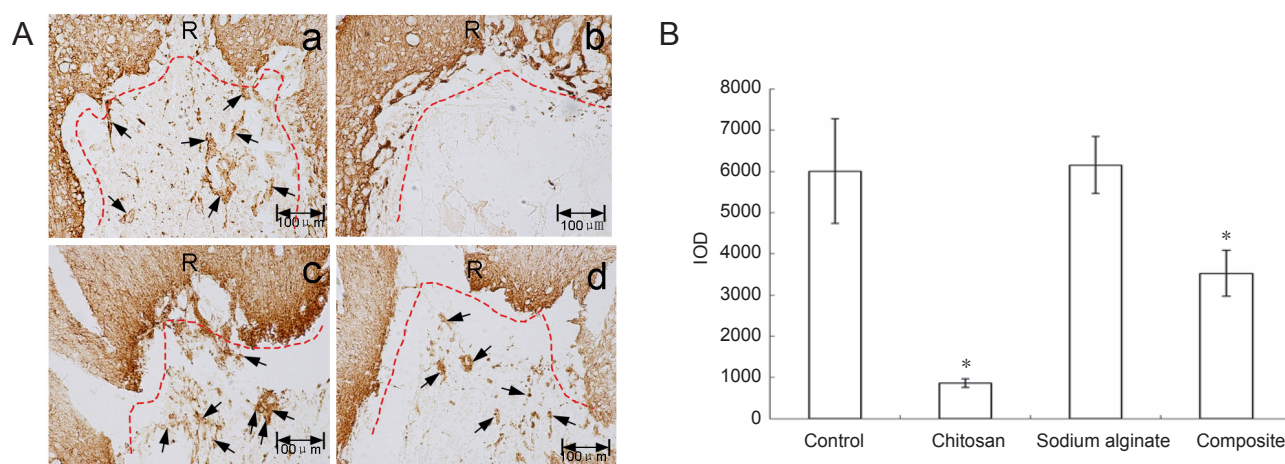


Figure 6 GFAP expression in the spinal cord injury site of experimental rats sixty days after surgery. (A) Immunohistochemical staining for GFAP protein; no scaffold (a), chitosan (b), sodium alginate (c), or chitosan-sodium alginate composite (d) scaffolds were implanted into the injury site of the rats. Sixty days after surgery, the spinal cords were excised, fixed, embedded in paraffin and stained with anti-GFAP antibody. The sections were photographed under a dissecting microscope. Red dotted lines mark the damage boundary; R is the injury rostral end; black arrows point to glial scar tissue. Scale bars: 100 μ m. (B) Quantitative analysis of GFAP expression (mean \pm SD, $n = 9$, one-way analysis of variance followed by the Student-Newman-Keuls *post hoc* test; * $P < 0.05$, vs. control group). Control: Control group; chitosan: chitosan scaffold group; sodium alginate: sodium alginate scaffold group; composite: composite material scaffold group. GFAP: Glial fibrillary acidic protein; IOD: integrated optical density.

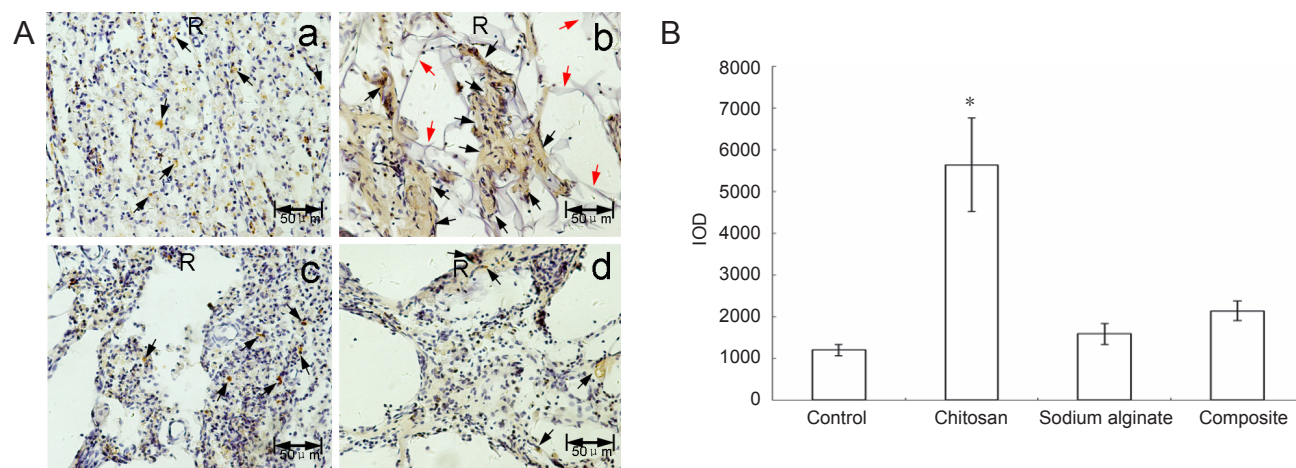


Figure 7 NF-H expression at the spinal cord injury site of experimental rats sixty days after surgery. (A) Immunohistochemical staining of NF-H protein; no scaffold (a), chitosan (b), sodium alginate (c), or chitosan-sodium alginate composite (d) scaffolds were implanted into the injury site of the rats. Sixty days after surgery, the spinal cords were excised, fixed, embedded in paraffin, stained with anti-NF-H antibody and restained with hematoxylin. The sections were photographed under a dissecting microscope. Brown represents NF-H immunoreactivity and purple represents nuclei. Black arrows point to NF-H immunoreactivity. Red arrows point to undegraded chitosan scaffold. Scale bars: 50 μ m. (B) Quantitative analysis of NF-H expression (mean \pm SD, $n = 9$, one-way analysis of variance followed by the Student-Newman-Keuls *post hoc* test; * $P < 0.05$, vs. control group). Control: Control group; chitosan: chitosan scaffold group; sodium alginate: sodium alginate scaffold group; composite: composite material scaffold group. NF-H: Neurofilament-H; IOD: integrated optical density.

NF-H immunohistochemical results are shown in **Figure 7A**. After restaining with hematoxylin, brown represented NF-H positive staining and purple represented nuclei. NF-H expression was dotted in the control and sodium alginate scaffold groups. NF-H expression was much greater, and flake-like nerve fibers were observed (black arrows) in the chitosan scaffold and composite material scaffold groups. NF-H expression was greater in the chitosan scaffold group than in the composite material scaffold group. **Figure 7B** shows the quantitative results obtained by randomly selecting three fields of NF-H immunohistochemistry in microphotographs, which

showed that NF-H expression was greatest in the chitosan scaffold group among the four experimental groups.

Discussion

A variety of cytokines can prevent axonal regeneration after SCI, but damage to the spinal cord can be restored with proper environmental conditions and regenerating spinal cord can grow through the damaged area to the distal side. Previous studies have verified the effectiveness of neural stem cell transplantation (Salewski et al., 2015; Zhang et al., 2016; Zhao et al., 2016a, b), peripheral nerve grafts and fetal

spinal cord transplantation (David and Aguayo 1981; Cheng et al., 1996), bone marrow mesenchymal stem cell transplantation (Zurita and Vaquero, 2006; Yin et al., 2014) and semi-liquid collagen injections (Joosten Bar and Gispén, 1995; Yoshii et al., 2003).

Chitosan [β -(1-4)-2-amino-2-deoxy-D-glucan], the deacetylated product of chitin, has many excellent properties, such as biocompatibility, biodegradability, and antibacterial and hemostatic activities (Chen et al., 2003; Itoh et al., 2003; Jarmila and Vavříková, 2011). These features make chitosan useful for tissue engineering research, and studies have shown that implantation of chitosan materials after SCI can promote axonal regeneration (Cho et al., 2010). Chitosan is often used as a delivery system or carrier for the recovery of SCI (Jian et al., 2015; Zhang et al., 2016).

Sodium alginate is natural polysaccharide extracted from brown algae that has good stability, solubility, viscosity, and biodegradability (Zhang et al., 2015). Sodium alginate gels can be formed when sodium alginate is crosslinked with Ca^{2+} *in vivo*, so sodium alginate can be made into a three-dimensional scaffold to support cell growth (Choi et al., 1999; Jon et al., 1999; Wang et al., 2012). Studies have shown that implantation of sodium alginate scaffolds has benefit for axonal regeneration after SCI (Prang et al., 2006; Wang et al., 2006). However, the composite scaffold of chitosan and sodium alginate has seldom been used for the recovery of SCI. Microcapsules of chitosan and sodium alginate have good biocompatibility (Song et al., 2004). Francis et al. (2013) made a type of ice-templated, linearly aligned chitosan-alginate scaffold, and this scaffold could support neuronal attachment and the linearly aligned growth of dorsal root ganglion neurites.

In the present study, chitosan scaffolds, sodium alginate scaffolds and composite scaffolds of chitosan-sodium alginate were prepared. The three kinds of scaffolds were porous sponges with good stability and flexibility in saline. SEM results showed that the surface structure of chitosan was the most compact and that of the composite material scaffold was the loosest.

In this experiment, the hemisection spinal cord model was established by dissecting approximately half of the spinal cord across its width from the right side. As a certain amount of left-side spinal cord and some blood vessels were removed when the spinal cord was damaged, the function of both hind limbs was affected, with similar results reported previously. After surgery, rat inertia was very strong and less food and water were consumed compared with normal rats. The postoperative condition of some rats became worse and some died; three and four rats died in the control and composite material scaffold groups, respectively. The death rate in the chitosan scaffold and sodium alginate scaffold groups was lowest. Obvious edema was observed at the injury site in the composite material scaffold group under a dissecting microscope. Taken together, the biocompatibility of chitosan scaffolds and sodium alginate scaffolds was good, preventing injury edema and reducing the death rate. This is possibly because of good biocompatibility and good recovery of movement function of the left hind limb in the chitosan scaffold and sodium alginate scaffold groups (8.6 in the chitosan scaffold group, 7.3 in the sodium alginate

scaffold group, and 5.3 in the control group). However, in the right hind limbs, the motor function recovery in the sodium alginate scaffold group (3.9) was less than that of the chitosan scaffold group (7.2); and there was no significant difference between the alginate scaffold group and control group (3.4). As the right-side spinal cord was dissected, the motor function recovery of right hind limbs mainly depended on the supporting and bridging roles of the scaffold. The degradation rate of the sodium alginate scaffold was so fast that no scaffold was observed at the injury site in the sodium alginate scaffold group and as such, it could not provide a supporting and bridging role. The spinal cord shape of the chitosan scaffold group was well-maintained and no atrophy was observed. Scaffolds for the repair of SCI should not only have a supporting role, but also should inhibit glial scar formation and mediate nerve cell growth.

GFAP is expressed in astrocytes and detection of its expression provides the position of the scar tissue. Results of immunohistochemistry for GFAP were consistent with the results of hematoxylin-eosin staining. There was a large number of glial cells at the injury site of control rats, which indicated severe glial scar formation. Conversely, almost no GFAP-immunoreactive cells were observed at the injury site in the chitosan scaffold group, indicating that the tissue among the chitosan pores was not scar tissue. It may have been nerve fibers and chitosan scaffolds prevented scar tissue entering the injury site. Some scar tissue was observed at the injury site in the sodium alginate scaffold and composite material scaffold groups, which may be because of the fast degradation rate of sodium alginate and the large pore in these two kinds of scaffolds.

NF-H is the heavy chain of neurofilament protein and an important component of nerve fibers. The nerve fibers observed at the injury sites exhibited dotted NF-H distribution in the control and sodium alginate scaffold groups, but were filiform in the chitosan scaffold and composite material scaffold groups. The number of nerve fibers was greater in the chitosan scaffold group than other groups, suggesting that chitosan scaffolds can promote the growth of nerve fibers.

In summary, due to the fast degradation rate of sodium alginate and composite material scaffolds, they could not play a good supporting and bridging role *in vivo*, but instead resulted in a large amount of scar tissue at the injury site, with resulting weak effects on spinal cord repair. Conversely, the degradation rate of chitosan scaffolds was slow and remained dense 60 days after surgery. Thus, chitosan scaffolds played a good supporting and bridging role. Moreover, chitosan scaffolds had good biocompatibility, not only inhibiting the formation of scar tissue, but mediating nerve regeneration and aiding the recovery after SCI.

Author contributions: ZAY and HGW designed the study. FJC, TL and NG performed experiments. ZAY and HLC analyzed data. HLC and HGW wrote the paper. All authors participated in the conception of this study and approved the final version of this paper.

Conflicts of interest: None declared.

Financial support: This work was supported by the National Natural Science Foundation of China, No. 81671243 and 81373429. Funders had no involvement in the study design; data collection, analysis, and interpretation; paper

writing; or decision to submit the paper for publication.

Research ethics: The experimental protocol was approved by the China Institutional Ethics Review Committee for Animal Experimentation (approval No. dlu2016022). The experimental procedure followed the United States National Institutes of Health Guide for the Care and Use of Laboratory Animals (NIH Publication No. 85-23, revised 1985).

Data sharing statement: Datasets analyzed during the current study are available from the corresponding author on reasonable request.

Plagiarism check: Checked twice by iThenticate.

Peer review: Externally peer reviewed.

Open access statement: This is an open access article distributed under the terms of the Creative Commons Attribution-NonCommercial-ShareAlike 3.0 License, which allows others to remix, tweak, and build upon the work non-commercially, as long as the author is credited and the new creations are licensed under identical terms.

Open peer reviewer: Changjong Moon, Chonnam National University, Republic of Korea.

References

- Austin JW, Kang CE, Baumann MD, DiDiodato L, Satkunendrarajah K, Wilson JR, Stanisz GJ, Shoichet MS, Fehlings MG (2012) The effects of intrathecal injection of a hyaluronan-based hydrogel on inflammation, scarring and neurobehavioural outcomes in a rat model of severe spinal cord injury associated with arachnoiditis. *Biomaterials* 33:4555-4564.
- Basso DM, Beattie MS, Bresnahan JC (1995) A sensitive and reliable locomotor rating scale for open field testing in rats. *J Neurotrauma* 12:1-21.
- Bolsover S, Fabes J, Anderson PN (2008) Axonal guidance molecules and the failure of axonal regeneration in the adult mammalian spinal cord. *Restorative Neurology & Neuroscience* 26:117-130.
- Cheng H, Cao Y, Olson L (1996) Spinal cord repair in adult paraplegic rats: partial restoration of hind limb function. *Science* 273:510-513.
- Cheng MY, Cao WL, Gao Y, Gong Y, Zhao N, Zhang X (2003) Studies on nerve cell affinity of biodegradable modified chitosan films. *J Biomater Sci* 14:1155-1167.
- Cheung RC, Ng TB, Wong JH, Chan WY (2015) Chitosan: an update on potential biomedical and pharmaceutical applications. *Mar Drugs* 13:5156-5186.
- Cho Y, Shi R, Borgens RB (2010) Chitosan produces potent neuroprotection and physiological recovery following traumatic spinal cord injury. *J Exp Biol* 213:1513-1520.
- David S and Aguayo AJ (1981) Axonal elongation into peripheral nervous system 'bridges' after central nervous system injury in adult rats. *Science* 214:931-933.
- Ding YM, Li YY, Wang C, Huang H, Zheng CC, Huang SH, Xuan Y, Sun XY, Zhang X (2017) Nischarin-siRNA delivered by polyethylenimine-alginate nanoparticles accelerates motor function recovery after spinal cord injury. *Neural Regen Res* 12:1687-1694.
- Faccendini A, Viganì B, Rossi S, Sandri G, Bonferoni MC, Caramella CM, Ferrari F (2017) Nanofiber scaffolds as drug delivery systems to bridge spinal cord injury. *Pharmaceuticals* doi: 10.3390/ph10030063.
- Figueiredo N (2017) Motor exam of patients with spinal cord injury: a terminological imbroglia. *Neurol Sci* 38:1159-1165.
- Francis NL, Hunger PM, Donius AE, Riblett BW, Zavaliangos A, Wegst UG, Wheatley MA (2013) An ice-templated, linearly aligned chitosan-alginate scaffold for neural tissue engineering. *J Biomed Mater Res A* 101:3493-503.
- Gulova I, Slovinska L, Blaško J, Devaux S, Wisztorski M, Salzet M, Fournier I, Kryukov O, Cohen S, Cizkova D (2015) Delivery of alginate scaffold releasing two trophic factors for spinal cord injury repair. *Sci Rep* 5:13702.
- Itoh S, Yamaguchi I, Suzuki M, Ichinose S, Takakuda K, Kobayashi H, Shinomiya K, Tanaka J (2003) Hydroxyapatite-coated tendon chitosan tubes with adsorbed laminin peptides facilitate nerve regeneration in vivo. *Brain Res* 993:111-123.
- Jarmila V, Vavřiková E (2011) Chitosan derivatives with antimicrobial, antitumor and antioxidant activities--a review. *Curr Pharm Des* 17:3596-3607.
- Jian R, Yixu Y, Sheyu L, Jianhong S, Yaohua Y, Xing S, Qingfeng H, Xiaojian L, Lei Z, Yan Z, Fangling X, Huasong G, Yilu G (2015) Repair of spinal cord injury by chitosan scaffold with glioma ECM and SB216763 implantation in adult rats. *J Biomed Mater Res A* 103:3259-3272.
- Jon AR, Gerard M, David JM (1999) Alginate hydrogels as synthetic extracellular matrix materials. *Biomaterials* 20:45-53.
- Joosten EA, Bar PR, Gispén WH (1995) Collagen implants and cortico-spinal axonal growth after mid-thoracic spinal cord lesion in the adult rat. *J Neurosci Res* 41:481-490.
- Kim M, Park SR, Choi BH (2014) Biomaterial scaffolds used for the regeneration of spinal cord injury (SCI). *Histol Histopathol* 29:1395-1408.
- Li G, Che MT, Zhang K, Qin LN, Zhang YT, Chen RQ, Rong LM, Liu S, Ding Y, Shen HY, Long SM, Wu JL, Ling EA, Zeng YS (2016) Graft of the NT-3 persistent delivery gelatin sponge scaffold promotes axon regeneration, attenuates inflammation, and induces cell migration in rat and canine with spinal cord injury. *Biomaterials* 83:233-248.
- Li XG, Yang ZY, Zhang AF, Wang TL, Chen WC (2009) Repair of thoracic spinal cord injury by chitosan tube implantation in adult rats. *Biomaterials* 30:1121-1132.
- Liu P, Zhao X (2013) Facile preparation of well-defined near-monodisperse chitosan/sodium alginate polyelectrolyte complex nanoparticles (CS/SAL NPs) via ionotropic gelification: a suitable technique for drug delivery systems. *Biotechnol J* 8:847-854.
- Nunamaker EA, Purcell EK, Kipke DR (2007) In vivo stability and biocompatibility of implanted Sodium alginate disks. *J Biomed Mater Res A* 83A:1128-1137.
- Prang P, Müller R, Eljaouhari A, Heckmann K, Kunz W, Weber T, Faber C, Vroemen M, Bogdahn U, Weidner N (2006) The promotion of oriented axonal regrowth in the injured spinal cord by alginate-based anisotropic capillary hydrogels. *Biomaterials* 27:3560-3569.
- Rabchevsky AG, Patel SP, Sullivan PG (2017) Targeting mitoNEET with pioglitazone for therapeutic neuroprotection after spinal cord injury. *Neural Regen Res* 12:1807-1808.
- Salewski RP, Mitchell RA, Li L, Shen C, Milekovskaia M, Nagy A, Fehlings MG (2015) Transplantation of induced pluripotent stem cell-derived neural stem cells mediate functional recovery following thoracic spinal cord injury through remyelination of axons. *Stem Cells Transl Med* 28:23-32.
- Saravanan S, Leena RS, Selvamurugan N (2016) Chitosan based biocomposite scaffolds for bone tissue engineering. *Int J Biol Macromol* 93:1354-1365.
- Song YP, Hu GH, Dong LH, Ma JH, Li SJ (2004) Immunoinhibition effect and biocompatibility of sodium alginate/chitosan. *Jilin Daxue Xuebao:(Yixueban)* 30:35-38.
- Subramanian A, Krishnan UM, Sethuraman S (2009) Development of biomaterial scaffold for nerve tissue engineering: Biomaterial mediated neural regeneration. *J Biomed Sci* 16:108.
- Sun X, Jones ZB, Chen X, Zhou L, So KF, Ren Y (2016) Multiple organ dysfunction and systemic inflammation after spinal cord injury: a complex relationship. *J Neuroinflammation* 13:260.
- Waibl H (1973) Zur Topographie der Medulla spinalis der Albinoratte (*Rattus norvegicus*). *Adv Anat Embryol Cell Biol* 47.
- Wang A, Ao Q, Cao W, Yu M, He Q, Kong L, Zhang L, Gong Y, Zhang X (2006) Porous chitosan tubular scaffolds with knitted outer wall and controllable inner structure for nerve tissue engineering. *J Biomed Mater Res A* 79:36-46.
- Wang CC, Yang KC, Lin KH, Liu YL, Liu HC, Lin FH (2012) Cartilage regeneration in SCID mice using a highly organized three-dimensional alginate scaffold. *Biomaterials* 33:120-127.
- Wen Y, Yu S, Wu Y, Ju R, Wang H, Liu Y, Wang Y, Xu Q (2016) Spinal cord injury repair by implantation of structured hyaluronic acid scaffold with PLGA microspheres in the rat. *Cell Tissue Res* 364:17-28.
- Yin F, Meng C, Lu R, Li L, Zhang Y, Chen H, Qin Y, Guo L (2014) Bone marrow mesenchymal stem cells repair spinal cord ischemia/reperfusion injury by promoting axonal growth and anti-autophagy. *Neural Regen Res* 9:1665-1671.
- Yoshii S, Oka M, Shima M, Akagi M, Taniguchi A (2003) Bridging a spinal cord defect using collagen filament. *Spine* 28:2346-2351.
- Zhang J, Lu X, Feng G, Gu Z, Sun Y, Bao G, Xu G, Lu Y, Chen J, Xu L, Feng X, Cui Z (2016) Chitosan scaffolds induce human dental pulp stem cells to neural differentiation: potential roles for spinal cord injury therapy. *Cell Tissue Res* 366:129-142.
- Zhang H, Zheng H, Zhang Q, Wang J, Konno M (2015) The interaction of sodium alginate with univalent cations. *Biopolymers* 46:395-402.
- Zhang W, Zhu XQ, Zhang DC (2016) Transplantation of bone marrow mesenchymal stem cells overexpressing Shootin1 for treatment of spinal cord injury. *Zhongguo Zuzhi Gongcheng Yanjiu* 20:7507-7517.
- Zhao XW, Liu X, Yu DP, Rong H, Yu XS, Yang CS, Liu T, Zhao TB (2016a) Partition-type spinal cord catheter combined with bone marrow stromal stem cells in the repair of spinal cord transection injury in rats. *Zhongguo Zuzhi Gongcheng Yanjiu* 20:42-48.
- Zhao Y, Zuo Y, Jiang J, Yan H, Wang X, Huo H, Xiao Y (2016b) Neural stem cell transplantation combined with erythropoietin for the treatment of spinal cord injury in rats. *Exp Ther Med* 12:2688-2694.
- Zurita M, Vaquero J (2006) Bone marrow stromal cells can achieve cure of chronic paraplegic rats: functional and morphological outcome one year after transplantation. *Neurosci Lett* 402:51-56.

(Copyedited by Turnley A, Norman C, Wang J, Li CH, Qiu Y, Song LP, Zhao M)